16th Australasian Fluid Mechanics Conference
Crown Plaza, Gold Coast, Australia
2-7 December 2007

Numerical Study of Droplet Generation in A Complex Micro-Channel

A. Bui and Y. Zhu

Microfluidics Laboratory, Thermal and Fluid Dynamics Group, CSIRO Division of CIP/CMMT,
PO Box 56, Highett, VIC 3190, AUSTRALIA

Abstract

Small liquid drops have many applications in science and technology. In microfluidics research, microscopic drops are used to facilitate micromixing, loading and dispensing reagents from micro-reactors, or to improve the efficiency of cell sorting and fluid sampling systems. Many factors can affect the micro-drop generation, such as fluid rheology, flow speed, and interaction of the fluid(gas)-fluid interface with the channel walls. In this paper, a numerical study of the generation of microscopic droplets in a micro-channel of complex geometry is presented. The multiphase flow with interface in complex micro-channel is described by a coupled immersed boundary and level-set front-capturing methods. Comparison of the simulation with experimental results is also presented.

Introduction

Water-in-oil microdrops are very promising for use as nano-reactors. The well-defined and isolated compartments allow the individual reaction in each drop free of contamination or disturbance by outside environment. The ever-increasing interests in droplet-based microfluidic technologies has triggered the recent increase in research activity in the area using both experimental and numerical methods[1, 13, 4, 7].

Numerical modelling of water-in-oil flow in microchannels is a challenging task due to the presence of fluid-fluid interfaces and the limitation of the analytical and numerical methods in dealing with complex geometries. To describe the complex evolution of the fluid-fluid interfaces either the 'Lagrangian', 'Eulerian' or 'hybrid' methods can be used. The Eulerian methods which keep track of the interface motion and deformation using either particle, volume, or functional trackers are computationally efficient as they do not require grid deformation or explicitly following the movement of the interface. As a result, they can easily deal with multiple interface system and topological changes of the interface which happen during interface break-up or coalescence. A method of interface tracking technique based on the use of a level function, which is smooth and is convected by underlying flow on the Eulerian stationary grid has been derived by Osher et al. [8]. To deal with complex geometries, an immersed boundary method [6, 5, 12] has been developed in stead of using body fitted grids. In this method, a forcing field is introduced into the flow, so that the desired velocity can be achieved at the virtual immersed boundaries. The method allows simulation of flows in complex geometries using simple rectangular computational meshes without a need of coordinate transformation or domain partition.

In this study, a numerical method will be presented to model two-phase flows with interfaces in complex geometries. The level-set front tracking method will be used which is coupled with a high-resolution Navier-Stokes solver to provide an accurate prediction of the interface movement. The method is used to investigate the drop generation in a microchannel.

Technical approach

Immersed boundary method

The immersed boundary method simplifies the representation of complex boundary geometries and boundary motion by using simple rectangular computational meshes. Essentially, a body force field is introduced and applied in the grid nodes in the vicinity of the boundaries, so that the chosen speed of boundary movement can be achieved. There are two methods to compute the virtual boundary forces based on the concepts of either (i) feedback forcing [6] or (ii) direct forcing [5, 12]. In this work, the method of direct forcing is employed which compared to the feedback forcing method does not require small computational time step and is more efficient for three-dimensional implementation.

The momentum equation of fluid flow is written as,

$$\frac{\partial \mathbf{u}}{\partial t} + \mathbf{u}\cdot\nabla\mathbf{u} = -\frac{\nabla P}{\rho} + \nu\nabla^2\mathbf{u} + \mathbf{f}, \tag{1}$$

where $\mathbf{u}$ is the velocity vector of the fluid, t is time, p is pressure, ρ is the fluid density and ν is the kinematic viscosity of fluid. The bold characters refer to vectors hereafter. The force field $\mathbf{f}$ determined by

$$\mathbf{f}(\mathbf{x}) = \mathbf{u}\cdot\nabla\mathbf{u} + \frac{\nabla P}{\rho} - \nu\nabla^2\mathbf{u} + \frac{\mathbf{V}-\mathbf{u}_o}{\Delta t} \quad with\ \mathbf{x}\in\Gamma \tag{2}$$

will impose the condition $\mathbf{u} = \mathbf{V}$ at the virtual boundary Γ.

Level set front-tracking method

Essentially, the level-set method employs a smooth level function, ϕ, to describe the interface separating two immiscible fluids [8, 9]. This level function is chosen as a signed distance function with the zero level set defining the interface location. The level function is positive in one fluid region and negative in the other one and its absolute value indicates the distance to the interface. The level function is convected by flow field via,

$$\phi_t + \mathbf{u}\cdot\nabla\phi = 0 \tag{3}$$

Since this function is smooth across the interface (unlike the fluid properties) the above convection equation can be solved with high-order accuracy and without introducing numerical oscillations. Using the level function, the steep changes of fluid properties across the interface can be smoothed out to minimize numerical oscillations in the solution of Navier-Stokes equations as follows,

$$\begin{aligned} \rho_\varepsilon &= \rho_1 + (\rho_2-\rho_1)\cdot H_\varepsilon(\phi) \\ \mu_\varepsilon &= \mu_1 + (\mu_2-\mu_1)\cdot H_\varepsilon(\phi), \end{aligned} \tag{4}$$

where H_ε is a regularization Heaviside functions and ε is a regularization parameter, via,

$$H_\varepsilon(d) = \begin{cases} 0 & \text{if } d < \varepsilon \\ \frac{d+\varepsilon}{2\varepsilon} + \frac{sin(\pi d/\varepsilon)}{2\pi} & \text{if } |d| \le \varepsilon \\ 0 & \text{if } d > \varepsilon. \end{cases} \tag{5}$$

Another major advantage of using the level function is that the geometric properties of the two-dimensional or three-dimensional interface, i.e. normal vector and surface curvature, can readily be determined from the level function as follows:

$$\mathbf{n} = \frac{\nabla\phi}{|\nabla\phi|}, \qquad k = \nabla\mathbf{n} = \nabla\cdot\frac{\nabla\phi}{|\nabla\phi|}. \tag{6}$$

The surface tension force appearing in the momentum equation can be defined in terms of the level function, via,

$$\mathbf{F}_s = \sigma k\delta(\phi)\mathbf{n} = \sigma\delta_\varepsilon(\phi)\cdot\nabla\phi\cdot\nabla\left(\frac{\nabla\phi}{|\nabla\phi|}\right), \tag{7}$$

where σ is the surface tension and $\delta_\varepsilon(\phi)$ is a delta function corresponding to H_ε, via,

$$\delta_\varepsilon(\phi) = \begin{cases} 0 & \text{if } |\phi| > \varepsilon \\ \frac{1}{2}[1+cos(\phi/\varepsilon)/\varepsilon] & \text{if } |\phi| \le \varepsilon. \end{cases} \tag{8}$$

The level set method can handle complex topological changes of the interface, such as breaking or merging, and its formulation is generic for two- and three-dimensional problems.

Description of the flow solver

To solve the system of the governing equations a two-step projection method is used. A pressure correction equation of the form

$$\nabla\left(\frac{1}{\rho}\cdot\nabla\delta p\right) = \frac{\nabla\mathbf{u}}{\Delta t} \tag{9}$$

is to be solved each time step using an iterative Generalized Minimum Residual (GMRES) solver. More details on the flow solver can be found in the work by Bui et al.[2].

Model validations and predictions

Validation of the immersed boundary model

The flow around a suddenly accelerated cylinder was investigated. A square domain of size 2 was discretized by a uniform 256×256 grid. The cylinder had a size of 0.44 in diameter and the cylinder was located at the centre of the computational domain. To create a start-up flow, a uniform velocity field was initialised in the domain and the initial flow Reynolds number was 550.

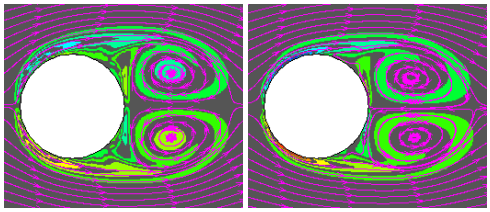

Figure 1: Streamlines and vorticity isolines of the flow around a suddenly accelerated cylinder at time t·U$_\infty$/R=5.12 obtained with the indirect (left) and direct (right) immersed boundary methods, respectively. Here R is the cylinder radius, U_∞ is the flow speed far away from the cylinder.

Figure 1 shows that both the direct and indirect immersed boundary methods produced primary vortices behind the cylinder whose sizes were comparable to the cylinder size. However, the flow streamlines seemed to attach more closely to the cylinder surface in the direct-forcing prediction in comparison with that from the indirect-forcing prediction. The difference is probably caused by the wider distribution of the forcing field from the virtual boundary in the indirect forcing method as opposed to the direct assignment of forces to much smaller number of points in the immediate vicinity to the boundary in the direct forcing method.

Validation of the level set front-tracking

Intensive validation of the level set front-tracking model had been done before (see [3] and [2]). The model was shown to be able to correctly predict the evolution of the interfaces during the process of bubble detachment and bursting.

Details of microchannel geometry for drop generation

For drop generation, a flow focusing technique was used which employed a cross-junction channel geometry. A picture of the microchip is shown in Figure 2. To form water in oil droplets, the water flow from the left channel was focused by the two side channels. The focused jet broke into microdrops by the shearing force of oil stream. The microchip was fabricated in a polycarbonate slide with dimensions of $75mm \times 25mm$ and a thickness of $2mm$. The microchip was fabricated in the CSIRO Microfabrication Laboratory, Clayton, VIC 3169, Australia. The droplet experiments were carried out in the CSIRO Microfluidics Laboratory at Highett, Melbourne, Australia. A photography technique was used to image droplets under a microscope and drop sizes were obtained by image analysis.

Figure 2: A picture of the microfluidic chip with water-in-oil droplets formed. The width of the channel at the cross was $105\mu m$ and the depth is $70\mu m$.

2D axisymmetric modelling of droplet generation

The developed model has been applied to study the generation of microdrops in a geometry which is similar to the experimental channel. In the axisymmetric simulations, the effects of the inlets larger than the realistic 3D counterparts and the so-called "focusing" of the radial flow when it approaches the axis of symmetry need to be taken into consideration, so that the desired fluid velocities in the droplet generation zone can be attained.

The simulations were conducted on a simple rectangular mesh with the complex channel geometry defined by the virtual immersed boundaries. Water was delivered through the axial inlet, while oil was entering the domain through the side inlets. Realistic fluid properties have been used and shown in Table 1. Since the oil viscosity is high, a semi-implicit scheme was employed for the viscous terms. The size of the computational grid was 64×284. The Reynolds numbers of the water and oil flows in the droplet generation zone were approximately 0.383 and 0.02, respectively.

Property	Water	Oil
Density ρ, kg/m^{-3}	1000	920
Viscosity μ, Pa·s	0.001	0.072
Surface tension σ, N/m	0.006 - 0.027	

Table 1: Fluid properties.

The modelling results are shown in Figures 3 to 6 for different flow conditions. For a given oil flow rate, an increase of surface tension resulted in an increase of droplet size but a decrease in the generation frequency. A reduction of the oil flow rate and hence the shear rate in the droplet generation zone effectuates

an increase of the droplet size. The above-mentioned relations obtained from the numerical simulations are found to be consistent with the previous experimental findings[4].

The droplet generation in the considered microfluidic channel is mainly driven by the shear force resulted from the oil flow. In such a condition, the size of the droplet generated can be estimated by equating the Laplace pressure with the shear force [4, 11]

$$d \sim \frac{\sigma}{\mu_o \dot{\gamma}} \tag{10}$$

where σ is the surface tension coefficient, μ_o is the oil viscosity and $\dot{\gamma}$ is the shear rate. Since the flows of oil and droplets occur in the same channel, the presence of a droplet of side d will result in a reduction of the channel cross-section by a factor of $[1-(d/D)^2]$ and an increase of the oil velocity and shear rate. Assuming that the cross-section of the droplet generation zone is a circle of diameter D, the following equation for droplet size can be derived from Eq. 10, via,

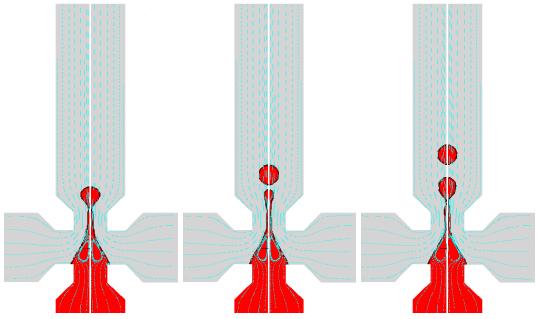

Figure 3: Flow streamlines and generation of droplets - $\sigma = 0.006 N/m$. The relative time t is in ms.

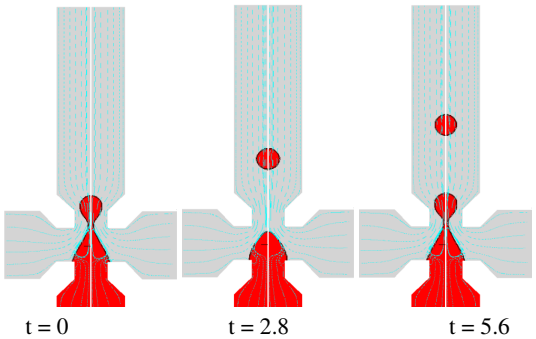

Figure 4: Flow streamlines and generation of droplets - $\sigma = 0.013 N/m$.

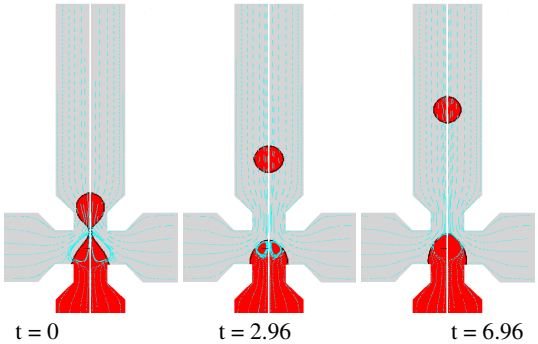

Figure 5: Flow streamlines and generation of droplets - $\sigma = 0.027 N/m$.

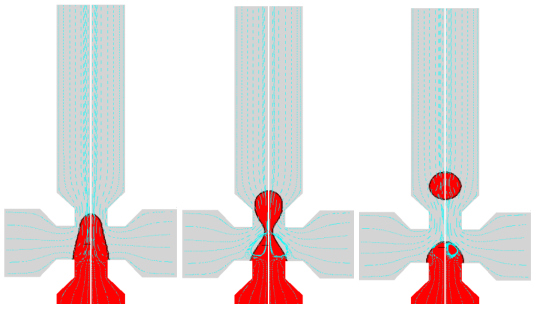

Figure 6: Flow streamlines and generation of droplets. Conditions same as above except that there was a 25% reduction of oil flow rate.

$$(D^2 - d^2)\cdot(D-d) = C \cdot \frac{\mu_o Q_o d}{\sigma} \tag{11}$$

where C is a constant and Q_o is the volumetric flow rate of the oil.

It is clear from Eq. 11 that the drop size is not simply proportional to σ or Q_o^{-1} as suggested by Eq.10. This fact was confirmed in a separate study presented in this conference by Zhu et al.[14]. Table 2 and Figure 7 indicate that Eq. 11 provides a better estimate of the droplet size as a function of surface tension and flow rate.

$\sigma, N/m$	CFD	Eqn. 11
0.006	50	69.5
0.013	64.6	78.6
0.027	81	84.8
0.027 - 25% Q_o reduction	85.6	86.8

Table 2: Droplet size in μm obtained from the CFD and Eq.11.

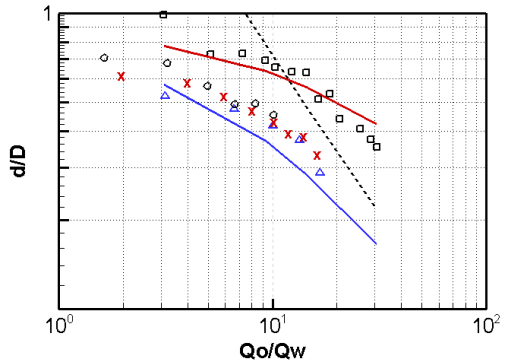

Figure 7: Experimental and analytical dependency of d/D on flow rate ratio Q_o/Q_w. []: CSIRO measurement [14]; $\triangle, \times, \circ$: Measurements by Tan et al.[10]; - -: Eq. 10; —,—: Eq. 11 for D equal 100 and 48μm, respectively.

3D modelling of droplet generation

The 3D modelling has been conducted on a $64\times284\times18$ rectangular mesh which covered a half of the real microfluidic channel. The channel depth was assumed to be 70μm. The inlet boundary conditions were adjusted so that the oil and water velocities remained the same in the droplet generation zone. In all simulations, the surface tension coefficient was 0.027 N/m. Figures 8-9 show the changes of the droplet shape and flow streamlines in time. Without a model to describe the effects of the contact angle, the contact lines are seen to slip freely along the walls and there is little change of the droplet shape in the third

dimension (channel depth). Consequently, the droplet could not detach from the neck as the curvature in the plane perpendicular to the channel axis and the centripetal surface tension force are very small. The 3D simulation result is similar to the predictions obtained with use of the commercial CFX-10 software with the wall contact model switched off (see Figure 9). Futher work is required to develop a method to account for the effects of the contact angle and the dynamics of the contact lines in the 3D model.

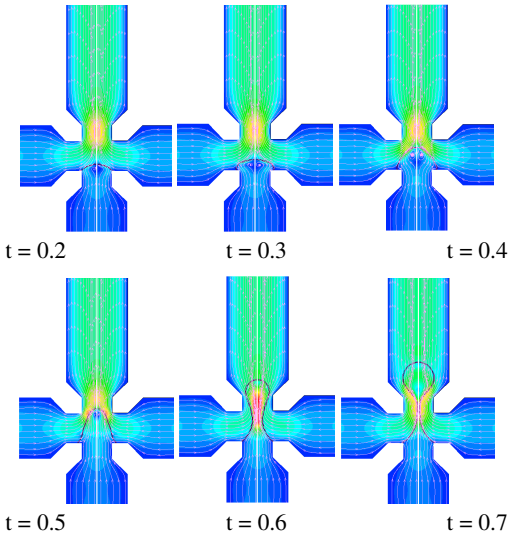

Figure 8: Flow streamlines and droplet surface at the central place. Unit for time is ms.

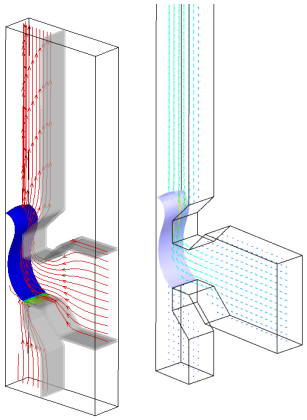

Figure 9: The shape of the droplet at 0.6ms compared with the corresponding CFX prediction.

Conclusions

In this work, a numerical model has been developed to simulate immiscible multiphase flows with interfaces in complex geometries. The model is based on the immersed boundary method to efficiently model the complex channel geometries and the level-set front-capturing method to keep track of the interface evolution. Coupled with a high-accuracy numerical scheme to solve the system of governing equations, the model is shown to be able to describe immiscible multiphase flows in complex channel geometries using simple rectangular grids. Both the immersed boundary and level set front-capturing methods have been validated separately and used to simulate the generation of droplets in a realistic microfluidic cross-chip. From the axisymmetric simulations, reasonable predictions of the trends of increase of droplet size with the increase of the surface tension and decrease of the oil flow rate were obtained. From the three-dimensional simulations, it is evident that correct prediction of the droplet generation could not be possible without a method to account for the effects of the contact angle and the dynamics of the contact lines. This issue is the subject of the future model development.

References

[1] Anna, S. L., Bontoux, N. and Stone, H. A., Formation of dispersions using flow focusing in microchannels, *App. Phys. Lett.*, **82**, 2003, 364–366.

[2] Bui, A. and Manasseh, R., A CFD study of the bubble deformation during detachment, Fifth International Conference on CFD in the Process Industries, Melbourne, Australia, 13-15 December, 2006, Paper 053, Paper 053.

[3] Bui, A. and Rudman, M., A numerical method for modelling of two-phase flow - solid interaction, Proceedings of 14th Aus. Fluid Mech. Conf., Adelaide 10-14 December, 2001.

[4] Cristini, V. and Tan, Y.-C., Theory and numerical simulation of droplet dynamics in complex flows-a review, *Lab on a Chip*, **4**, 2004, 257–264.

[5] Fadlun, E., Verzicco, R., Orlandi, P. and Mohd-Yusof, Combined immersed-boundary finited-difference methods for three-dimensional complex flow simulations, *J. Comp. Phys.*, **161**, 2000, 35–60.

[6] Goldstein, D., Handler, R. and Sirovich, L., Modeling a no-slip flow boundary with an external force field, *J. Comp. Phys.*, **105**, 1993, 354–366.

[7] Link, D. R., Grasland-Mongrain, E., Duri, A., Sarrazin, F., Cheng, Z., Cristobal, G., Marquez, M. and A.Weitz, D., Electric control of droplets in microfluidic devices, *Angew. Chem. Int. Ed.*, **45**, 2006, 2556–2560.

[8] Osher, S. and Sethian, J., Fronts propagating with curvature-dependent speed: algorithms based on hamilton-jacobi formulations, *J. Comp. Phys.*, **79**, 1988, 12–49.

[9] Sussman, M. and Puckett, E., A coupled level set and volume-of-fluid method for computing 3D and axisymmetric incompressible two-phase flows, *J. Comp. Phys.*, **162**, 2000, 301–337.

[10] Tan, Y.-C., Cristini, V. and Lee, A. P., Monodispersed microfluidic droplet generation by shear focusing microfluidic device, *Sensors and Actuators B*, **114**, 2006, 350–356.

[11] Taylor, G. I., The formation of emulsions in definable fields of flow, *Proc. Roy. Soc. Lond. A*, **146**, 1934, 501–523.

[12] Yakhot, A., Ginberg, L. and Nikitin, N., Modeling rough stenoses by an Immersed-Boundary method, *J. Biomech.*, **38(5)**, 2005, 1115–1127.

[13] Zheng, B., Roach, L. S. and Ismagilov, R. F., Screening of protein crystallization conditions on a microfluidic chip using nanoliter-size droplets, *J. Am Chem. Soc.*, **125**, 2003, 11170–11171.

[14] Zhu, Y., Noui-Mehidi, M. N., Leech, P. W., Sexton, B. A., Brown, S., Wu, N. and Easton, C., Droplets transport in a microfluidic chip for In Vitro compartmentalisation, Proceedings of 16th Aus. Fluid Mech. Conf., Queensland, 2007.